OPEN ACCESS

Original research

Airway epithelial cell response to RSV is mostly impaired in goblet and multiciliated cells in asthma

Aurore C A Gay ,[1,2] Martin Banchero,[1,2] Orestes Carpaij ,[2,3] Tessa M Kole ,[2,3] Leonie Apperloo,[1,2] Djoke van Gosliga,[2,4] Putri Ayu Fajar,[1,2] Gerard H Koppelman,[2,4] Louis Bont,[5,6] Rudi W Hendriks,[7] Maarten van den Berge,[2,3] Martijn C Nawijn[1,2]

► Additional supplemental material is published online only. To view, please visit the journal online (http://dx.doi.org/10.1136/thorax-2023-220230).

For numbered affiliations see end of article.

Correspondence to
Dr Martijn C Nawijn, Department of Pathology and Medical Biology, University Medical Center Groningen, Groningen Research Institute for Asthma and COPD, Groningen, 9713GZ, the Netherlands; m.c.nawijn@umcg.nl

Received 10 March 2023
Accepted 27 November 2023
Published Online First 19 February 2024

ABSTRACT

Background In patients with asthma, respiratory syncytial virus (RSV) infections can cause disease exacerbation by infecting the epithelial layer of the airways, inducing subsequent immune response. The type I interferon antiviral response of epithelial cells upon RSV infection is found to be reduced in asthma in most—but not all—studies. Moreover, the molecular mechanisms causing the differences in the asthmatic bronchial epithelium in response to viral infection are poorly understood.

Methods Here, we investigated the transcriptional response to RSV infection of primary bronchial epithelial cells (pBECs) from patients with asthma (n=8) and healthy donors (n=8). The pBECs obtained from bronchial brushes were differentiated in air-liquid interface conditions and infected with RSV. After 3 days, cells were processed for single-cell RNA sequencing.

Results A strong antiviral response to RSV was observed for all cell types, for all samples (p<1e-48). Most (1045) differentially regulated genes following RSV infection were found in cells transitioning to secretory cells. Goblet cells from patients with asthma showed lower expression of genes involved in the interferon response (false discovery rate <0.05), including *OASL*, *ICAM1* and *TNFAIP3*. In multiciliated cells, an impairment of the signalling pathways involved in the response to RSV in asthma was observed.

Conclusion Our results highlight that the response to RSV infection of the bronchial epithelium in asthma and healthy airways was largely similar. However, in asthma, the response of goblet and multiciliated cells is impaired, highlighting the need for studying airway epithelial cells at high resolution in the context of asthma exacerbation.

WHAT IS ALREADY KNOWN ON THIS TOPIC

⇒ The airway epithelium response to respiratory syncytial virus (RSV) is altered in asthma. However, literature remains conflicted about the exact changes in the antiviral response, and the mechanisms causing these changes are yet to be found.

WHAT THIS STUDY ADDS

⇒ This study describes extensively the response of the bronchial epithelial cells (BECs) to RSV for both healthy subjects and patients with asthma, at a single-cell resolution. It highlights the major overlap between healthy and asthma in the antiviral response to RSV. It allows the identification of specific genes and cell types that show a different behaviour in response to RSV in asthma compared with healthy.

HOW THIS STUDY MIGHT AFFECT RESEARCH, PRACTICE OR POLICY

⇒ Our study indicates that goblet and multiciliated cells are the most relevant BECs to further investigate in the context of drug development for RSV-induced asthma exacerbation. It also suggests that focusing research on the cross-talk between the epithelial and the immune cells, or into investigating a potential delayed response in asthma would be the best way forward into understanding the mechanisms involved in the asthma response to RSV.

INTRODUCTION

The prevalence of asthma, one of the major respiratory diseases worldwide, has increased in recent decades.[1] Asthma exacerbation remains a frequent cause for medical emergencies, and as such, a heavy burden on our healthcare systems.[2] In addition, frequent exacerbation results in subsequent asthma-associated loss of quality of life. Much of the asthma exacerbation is triggered by allergens or viral respiratory tract infection, with studies reporting respiratory syncytial virus (RSV) as an important viral cause for asthma exacerbation in adults.[3]

The airway epithelium acts as the primary defence against pathogens, and therefore represents the primary target for RSV infection. In asthma, the airway epithelium is more susceptible for injury and displays a reduced barrier function. The airway epithelium in asthma has a decreased expression of E-cadherin and tight junction proteins, together with an increased basal cell proportion.[4] These changes of the airway epithelium are thought to contribute to the impaired barrier formation in asthma that was reported in in vitro cultured bronchial epithelial cells.[5] In addition, studies indicated that the receptors involved in viral sensing were altered for individuals with asthma.[6] In particular, a decreased expression of pattern recognition receptors (PRRs) was observed in both patients with mild and severe asthma,[7] contributing to an increased susceptibility to viral infection for people with the disease.[8 9]

Check for updates

To cite: Gay ACA, Banchero M, Carpaij O, *et al*. *Thorax* 2024;**79**:811–821.

RSV binds to airway epithelial cells through the association of the viral attachment glycoprotein with glycosaminoglycans linked to transmembrane proteins at the cell surface. The viral entry is then facilitated by the viral fusion glycoprotein.[10] Though the main host cell attachment factor interacting with the viral fusion protein is thought to be the fractalkine receptor CX3C-chemokine receptor 1 (CX3CR1), several other proteins have been proposed to facilitate the RSV entry to the cell, such as the intercellular adhesion molecule 1 (ICAM1), the epidermal growth factor receptor (EGFR) and nucleolin.[10] Subsequent release of the viral RNA into the cytoplasm will activate two main PRRs: the Toll-like receptors and retinoic acid-inducible gene I-like receptor family members.[11] This triggers an early innate immune response activating type I and type II interferon and the nuclear factor kappa B (NF-κB) pathway.[9] In air-liquid interface (ALI) cultures derived from primary bronchial epithelial cells (pBECs) from patients with asthma, an exuberant inflammatory cytokine response was observed after RSV infection.[4] However, literature remains conflicted on the actual changes happening in the viral response to respiratory infection in the asthmatic airway. Several studies reported that type I interferon (IFN) production and the subsequent IFN response were reduced in the asthmatic airway after rhinovirus or RSV exposure, compared with airways from healthy controls.[12–15] However, others found that this antiviral response was preserved in pBECs in asthma,[16] or delayed,[17] compared with pBECs from healthy subjects. Those inconsistencies in the previous findings could be explained by differences in the response to RSV from the various cell types of the airway epithelium.

To this day, virally induced exacerbation of asthma remains difficult to prevent. Despite the importance of RSV in asthma exacerbation, the molecular mechanisms and cell type-specific responses that cause differences in the bronchial epithelial response to viral infection between healthy individuals and patients with asthma remain incompletely understood. Previous investigations of these mechanisms using bulk transcriptomics could not unveil cell specificity, and these unmeasured differences in cell type composition could partly explain the inconsistency observed in the current literature. In this study, we aimed therefore to compare the transcriptional response of pBECs in a cell type-specific fashion, between patients with asthma and healthy donors with RSV infection. After establishing the characteristics of our culture model in healthy and asthma-derived samples at baseline, we investigated the transcriptional response to RSV in the healthy-derived cultures and compared it with that of the asthma-derived cultures.

METHODS

Full methods are provided in the online supplemental file 1.

Subjects

We included samples derived from bronchial brushes from patients with asthma and from healthy controls as previously described.[18] The healthy donors showed normal lung function, defined as forced expiratory volume in 1 s (FEV_1)/forced vital capacity lower limit of normal, FEV_1 >80% predicted, an absence of bronchial hyper-responsiveness to methacholine (provocative concentration causing a 20% fall in FEV_1 methacholine mg/mL) and no allergies (see table 1 for subject characteristics). The patients with asthma had a confirmed diagnosis of asthma with either at least 12% and 200 mL reversibility of FEV_1 or fall in FEV_1 of at least 20% at <8 mg/mL methacholine (hyper-responsiveness). Patients were in GINA treatment steps 1–4, and not on oral corticosteroids, macrolides or biologicals when entering the study. After giving informed consent, patients were asked to stop using inhaled corticosteroid for a period of at least 6 weeks before follow-up tests and bronchoscopy. During this time, the patients only used short-acting beta-agonists.

Table 1 Clinical characteristics of the study cohort

	Asthma (n=8)	Healthy (n=8)	P value
Age	50.62 (9.56)	56.12 (7.68)	0.225
Sex=male	4	4	1.000
Smoking=past smoker	0	4	0.083
FEV_1 %predicted	94.25 (14.55)	114.12 (5.46)	0.003
FEV_1/FVC %	72.21 (8.53)	79.29 (3.74)	0.050
PC20 methacholine mg/mL	2.19 (1.95)	Not reached	
Blood eosinophil count $\times 10^9$/L	0.17 (0.13–0.27)	0.15 (0.11–0.19)	0.429

Age, FEV_1, FEV_1/FVC and PC20 are all presented as mean (SD) and tested with t-tests; blood eosinophil count as median (IQR) and tested with Mann-Whitney U test; the categorical variables (sex and smoking status) were tested with X^2 test. At the time of the bronchoscopy, no subjects were under any corticosteroid treatment (see the Methods section and online supplemental methods).
FEV_1, forced expiratory volume in 1 s; FVC, forced vital capacity; PC20, provocative concentration causing a 20% fall in FEV_1.

Healthy control subjects were not on immunomodulatory drugs such as oral corticosteroids. Both patients with asthma and healthy control subjects were recruited specifically for this clinical study, and as part of the protocol, all participants underwent a bronchoscopy for research purposes only, which was performed at least 6 weeks after stopping inhaled corticosteroids.

Additional details about the patient cohort can be found in the online supplemental material.

Culture of pBECs

pBECs were grown from bronchial brushes and differentiated in ALI cultures. During the fourth week of culture, cells were infected with RSV and were processed for single-cell RNA sequencing (scRNAseq) after 72 hours. ELISA was performed on the apical washes of the cultures as described in the online supplemental material.

Single-cell RNA sequencing

Library preparation and sequencing

Each sample was incubated individually with 0.025 µg TotalSeq-B hashtag antibodies (BioLegend, cat#: 394631, 394633, 394635 and 394637), according to the manufacturer's recommendation, and 4000 cells per sample (RSV or control) were pooled per 4 samples. Resulting cell suspensions were loaded and libraries were prepared according to standard protocol of the chromium single-cell 3' kit V.3.1 with Feature barcoding antibodies (10X Genomics). Quality and concentrations of the different libraries were assessed on TapeStation (Agilent). Gene expression libraries were sequenced on a Novaseq 6000 System (Illumina), aiming for 20 000 read pairs per cell, and cell surface protein libraries were sequenced on the NextSeq 550 System (Illumina), aiming for 5000 read pairs per cell, according to the manufacturer's recommendation.

Computational analysis

Data were aligned using cellRanger V.6.1.1 (10X Genomics) to the GRCh38 reference and the RSV genome (GCA_002815475.1), using a cut-off of minimum 500 UMIs to be considered as a cell Ambient RNA was corrected using FastCAR (https://github.

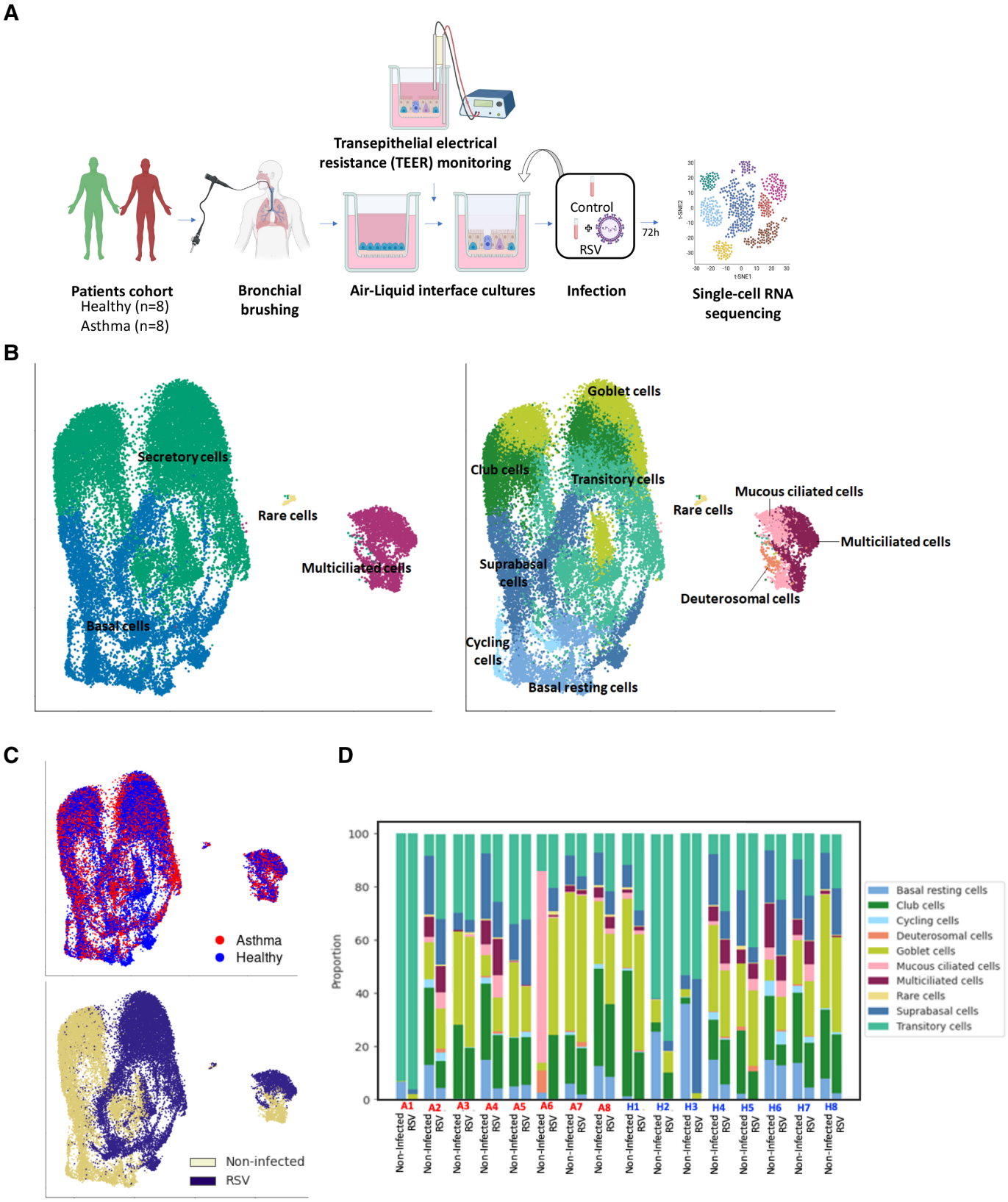

Figure 1 Experimental design and dataset overview. (A) Overview of the study design. BECs were obtained from healthy subjects and patients with asthma by bronchial brushes, and were differentiated in ALI cultures for 3 or 4 weeks before being treated with RSV. Cells were harvested and processed for scRNAseq. (B) UMAP representation of 30 604 single cells from all donors and conditions, clustered and annotated in 4 groups (left) and 10 subgroups (right), (C) coloured by disease (top) and treatment condition (bottom). (D) Proportions of cell types for each sample, calculated with scCODA. ALI, air-liquid interface; BECs, bronchial epithelial cells; RSV, respiratory syncytial virus; scRNAseq, single-cell RNA sequencing; UMAP, Uniform Manifold Approximation and Projection.

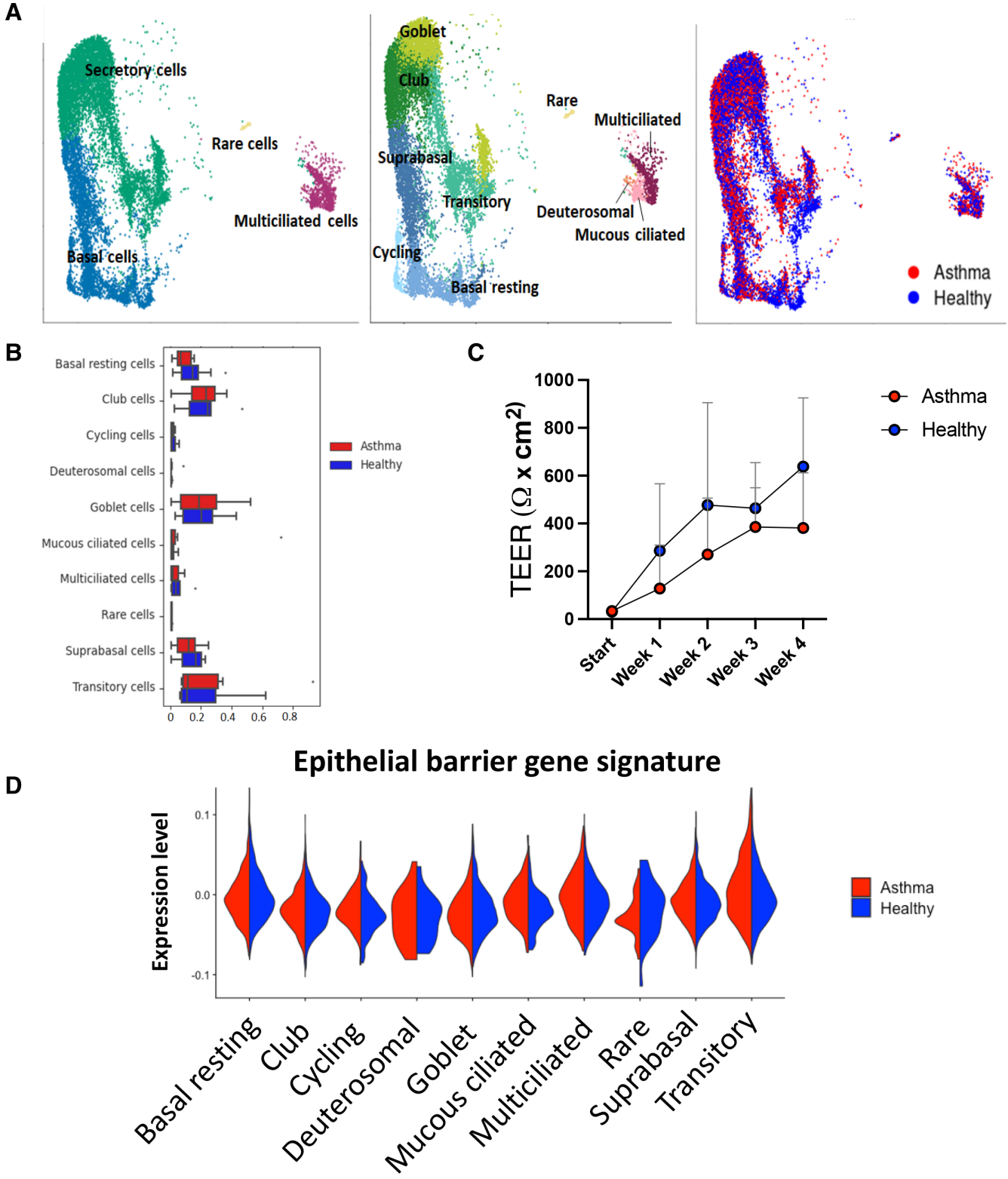

Figure 2 Similarities in cellular composition, barrier formation and transcriptional profiles between the ALI cultures derived from the patients with asthma and the ones derived from healthy subjects. (A) UMAP representation of untreated 7089 from untreated control and 6382 asthma cells, coloured by cell type (left), cell subtype (middle) and disease status (right). (B) Cellular frequencies of each cell subtype, coloured by disease status. Significance was determined by scCODA with an FDR-adjusted p<0.05. (C) TEER of the ALI cultures through time. Data are presented as mean±SD, comparisons between patient groups at a single time point were analysed using the Wilcoxon rank-sum test. Comparisons between two time points within the same group were done using two-way analysis of variance test. (D) Violin plots of the composite score of the genes involved in the epithelial barrier. ALI, air-liquid interface; FDR, false discovery rate; TEER, transepithelial electrical resistance; UMAP, Uniform Manifold Approximation and Projection.

Table 2 Overview of the number of cells in the scRNAseq dataset per donor per condition, for the pBECs derived from the healthy donors (top) and the patients with asthma (bottom), after quality control

	Number of cells	
	Control	RSV
Donors (healthy)		
H1	219	248
H2	1105	1024
H3	960	767
H4	1692	2156
H5	135	478
H6	1307	1986
H7	1352	1922
H8	319	628
Total	7089	9199
Donors (asthma)		
A1	195	319
A2	1976	2095
A3	179	218
A4	1505	1710
A5	662	767
A6	36	204
A7	729	689
A8	1100	1932
Total	6382	7934

RSV, respiratory syncytial virus; scRNAseq, single-cell RNA sequencing.

com/Nawijn-Group-Bioinformatics/FastCAR), using the recommend.empty.cutoff function for each sample, after generating the ambient profile according to the standard parameters.[19] Demultiplexing was performed using Seurat V.4.1.1[20] and SoupOrCell (https://github.com/wheaton5/souporcell).[21] Before integration, data were log-transformed, and the top 2000 highly variable features were selected. Integration was performed with FastMNN[22] to correct for the experimental batch effect. Clustering was performed using a k-nearest neighbour approach using the first 30 principal components (PCs) of the highly variable genes, and visualisation was performed by running the Uniform Manifold Approximation and Projection (UMAP) dimensional reduction technique, on the first 30 PCs in the highly variable genes of the data.

Cell type frequencies were calculated using scCODA (https://github.com/theislab/scCODA).[23] Differential gene expression (DGE) analysis was done using edgeR V.3.36.0[24] after generating a pseudobulk dataset per donor per condition for each cell type separately. Briefly, the counts were normalised by using the TMM method, after which, a quasi-likelihood binomial generalised log-linear (glmQL) model was applied and Benjamini-Hochberg correction was applied. For the DGE analysis comparing RSV condition with non-infected, we performed a paired analysis, to account for the correlated nature of the cells obtained from the same subject. For the interaction analysis, the following contrast was performed: $(\text{asthma}_{\text{RSV}} - \text{asthma}_{\text{non-infected}}) - (\text{healthy}_{\text{RSV}} - \text{healthy}_{\text{non-infected}})$. Gene Ontology (GO) analysis was conducted with g:Profiler and further visualisation was realised for the enriched pathways from the GO:BP database. Gene Set Enrichment Analysis (GSEA) was performed using fgsea (https://github.com/ctlab/fgsea), using the gene set collections from the V.7.4 of the Molecular Signatures Database. Cell–cell communication analysis was done with CellChat V.1.1.3 (https://github.com/sqjin/CellChat).[25]

Statistical analysis

Comparisons between patient groups at a single time point were analysed using the non-parametric Wilcoxon rank-sum test for paired observations. Comparisons between two time points within the same group were done using two-way analysis of variance test, using GraphPad Prism V.9.3.1 (https://www.graphpad.com).

Data availability and code reproducibility

All data is available at: https://ega-archive.org/studies/EGAS00001007450.

For reproducibility of the results, see https://github.com/Nawijn-Group-Bioinformatics/ALI-RSV_Reproducibility.

RESULTS

Cellular composition of primary epithelial cells differentiated in ALI cultures

To compare the cell type-specific response to RSV between pBECs obtained from patients with asthma and healthy controls, we infected pBECs from ALI cultures with RSV, and processed the cultures for scRNAseq 72 hours post-infection (hpi) (figure 1A). In total, we generated a dataset of 30 604 cells. Unsupervised clustering identified four main epithelial cell types in the ALI cultures: basal, secretory, multiciliated and rare cells (figure 1B). Subclustering at higher granularity allowed the identification of 10 different subsets of epithelial cells, including well-known or previously described subsets,[18 26] such as suprabasal, club and goblet cells, as well as deuterosomal and mucous ciliated cells (figure 1B).

RSV infection, but not disease status of the donor (healthy or asthma), caused a strong transcriptional change for each cell type as evident from the UMAP plots (figure 1C). For all donors, all types of basal and secretory cells were observed, but multiciliated cells were not present in all cultures (figure 1D).

Cellular composition, transcriptional profile and barrier formation are similar between the ALI cultures derived from the patients with asthma and the ones derived from healthy subjects

To assess whether the ALI cultures of pBECs derived from healthy subjects and patients with asthma displayed any differences at baseline, we compared the transcriptomic profiles of the non-infected cells between these two groups.

For both groups, all epithelial cell subsets were identified (figure 2A), with no differences in relative proportions (figure 2B). Cell type-specific DGE analysis revealed no significantly differentially expressed genes (DEGs) between the two groups in any of the cell types, and no pathways were found enriched in the subsequent GSEA, indicating that the epithelial cell phenotypes were very similar. The expression levels of *CX3CR1*, *EGFR*, *IGF1R*, *NCL* and *ICAM1,* all known to facilitate RSV entry to the cells,[10 27] were also similar (online supplemental figure 1). The same was observed for *DDX58* and *IFIH1*, encoding RIG-I-like receptors involved in sensing of viral RNA and the subsequent antiviral response.[28]

For both healthy-derived and asthma-derived ALI cultures, transepithelial electrical resistance (TEER) values increased

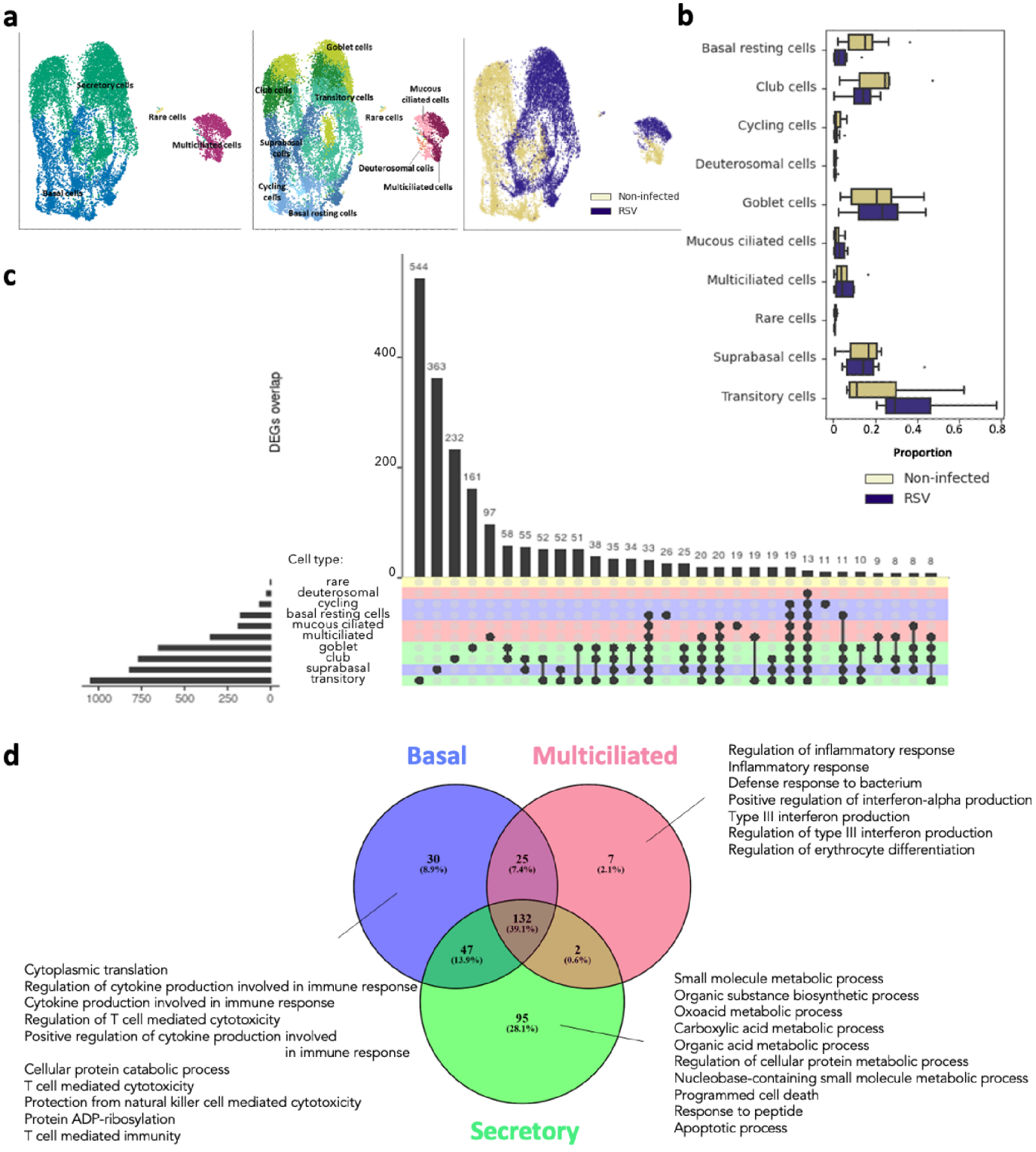

Figure 3 RSV infection induces transcriptomic changes in ALI-cultured pBECs derived from healthy subjects. (A) UMAP representation of untreated 7089 from untreated and 9199 RSV-infected cells, coloured by cell subtype (left) and treatment (right). (B) Cellular frequencies of each cell subtype, coloured by treatment. Significance was determined by scCODA with an FDR-adjusted p<0.05. (C) UpSet plot depicting the unique and shared sets of DEGs with RSV infection among cell subtypes. An FDR of less than 0.05 was considered as statistically significant. (D) Venn diagram of the biological processes found to be significantly enriched by GO analysis of the genes differentially expressed in RSV compared with control, in basal, secretory and multiciliated cells. The 10 most enriched processes are indicated. ALI, air-liquid interface; DEGs, differentially expressed genes; FDR, false discovery rate; GO, Gene Ontology; pBECs, primary bronchial epithelial cells; RSV, respiratory syncytial virus; UMAP, Uniform Manifold Approximation and Projection.

Table 3 GO analysis of the 148 genes found differentially expressed between untreated and RSV-infected samples and shared between basal, secretory and multiciliated lineages

Biological process (GO database)	Term ID	Adjusted p value
Response to other organisms	Go:0051707	9.461725873081114e-49
Defence response to virus	Go:0051607	1.0256624683287585e-48
Response to external biotic stimulus	Go:0043207	1.0928882461590793e-48
Defence response to symbiont	Go:0140546	1.2024119388813918e-48
Biological process involved in interspecies interaction between organisms	Go:0044419	4.990278548577266e-48
Response to biotic stimulus	Go:0009607	6.60851840516966e-48
Response to virus	Go:0009615	1.630041211843226e-47
Defence response to other organisms	Go:0098542	2.234003461280931e-46
Innate immune response	Go:0045087	1.0338142206864037e-43
Defence response	Go:0006952	3.994466335780032e-43
Immune response	Go:0006955	6.899998050993308e-37
Response to external stimulus	Go:0009605	7.385110179795586e-37
Immune system process	Go:0002376	1.9919579659955983e-30
Regulation of viral process	Go:0050792	7.273287357780607e-30
Negative regulation of viral process	Go:0048525	1.083345310148469e-29
Regulation of viral life cycle	Go:1 903 900	2.1337332693546325e-28
Response to stress	Go:0006950	6.4933736039781e-27
Regulation of response to biotic stimulus	Go:0002831	1.0780413145692529e-26
Viral process	Go:0016032	2.2219406695936574e-24
Negative regulation of viral genome replication	Go:0045071	1.305438220320424e-23
Regulation of viral genome replication	Go:0045069	2.6988811960322766e-23
Regulation of defence response	Go:0031347	3.059433362307539e-23
Response to cytokine	Go:0034097	1.301887546010741e-22
Response to type I interferon	GO:0034340	7.281206747097304e-22
Viral life cycle	Go:0019058	1.3834154909898275e-21

The 25 most enriched processes are displayed.
GO, Gene Ontology; RSV, respiratory syncytial virus.

over time, indicating the formation of an epithelial barrier. No significant difference was observed between the two groups (figure 2C), and the expression of a signature of genes involved in the epithelial barrier[29] was also similar between asthma and healthy ALIs (figure 2D).

RSV infection induces a strong immune response in pBECs from healthy donors

We then investigated the response of healthy control-derived ALI cultures of pBECs to RSV. We obtained 7089 control-treated cells and 9199 RSV-infected cells from the healthy donors (table 2), and all 10 subtypes of epithelial cells were identified in both conditions (figure 3A). No significant changes in cell-type proportions were observed in the samples infected with RSV compared with control treatment (figure 3B). In addition, no changes in TEER or in expression level of a signature of epithelial barrier genes[29] were observed after RSV infection (online supplemental figure 2A and C).

For each cell type, we identified the genes differentially expressed after RSV infection in cultured epithelial cells (figure 3C and online supplemental table 1). Cells transitioning from suprabasal to secretory cells had the highest number of DEGs (1045). GO analysis of the 148 DEGs shared between basal, secretory and ciliated cells in response to RSV revealed an enrichment of biological processes such as response to virus and cytokine production (table 3 and online supplemental table 2), indicating that the RSV infection triggered a proinflammatory and antiviral response from all three different types of epithelial cells.

GO analysis of the DEGs in basal, secretory and ciliated epithelial cells separately revealed cell type-specific effects of RSV infection: the type III IFN response was enriched after RSV infection, but statistically significant only in multiciliated cells (figure 3D and online supplemental table 2). Biological processes related to T cell-mediated immunity were exclusively found enriched in the basal cells, while many metabolic processes were only observed for the secretory cells.

Cell–cell communication analysis, using CellChat, showed that RSV infection induced an increase in number of intercellular interactions from all cell types (online supplemental figure 3A). Most cell–cell interactions were predicted to be stronger in the RSV-infected condition. We found that compared with untreated cells, many key signalling pathways were enriched for in the RSV-infected cells (online supplemental figure 3B). Among those, SEMA6, TGFb, IL1, ANGPTL, TRAIL and the DESMOSOME signalling pathways were essentially not present in the untreated condition.

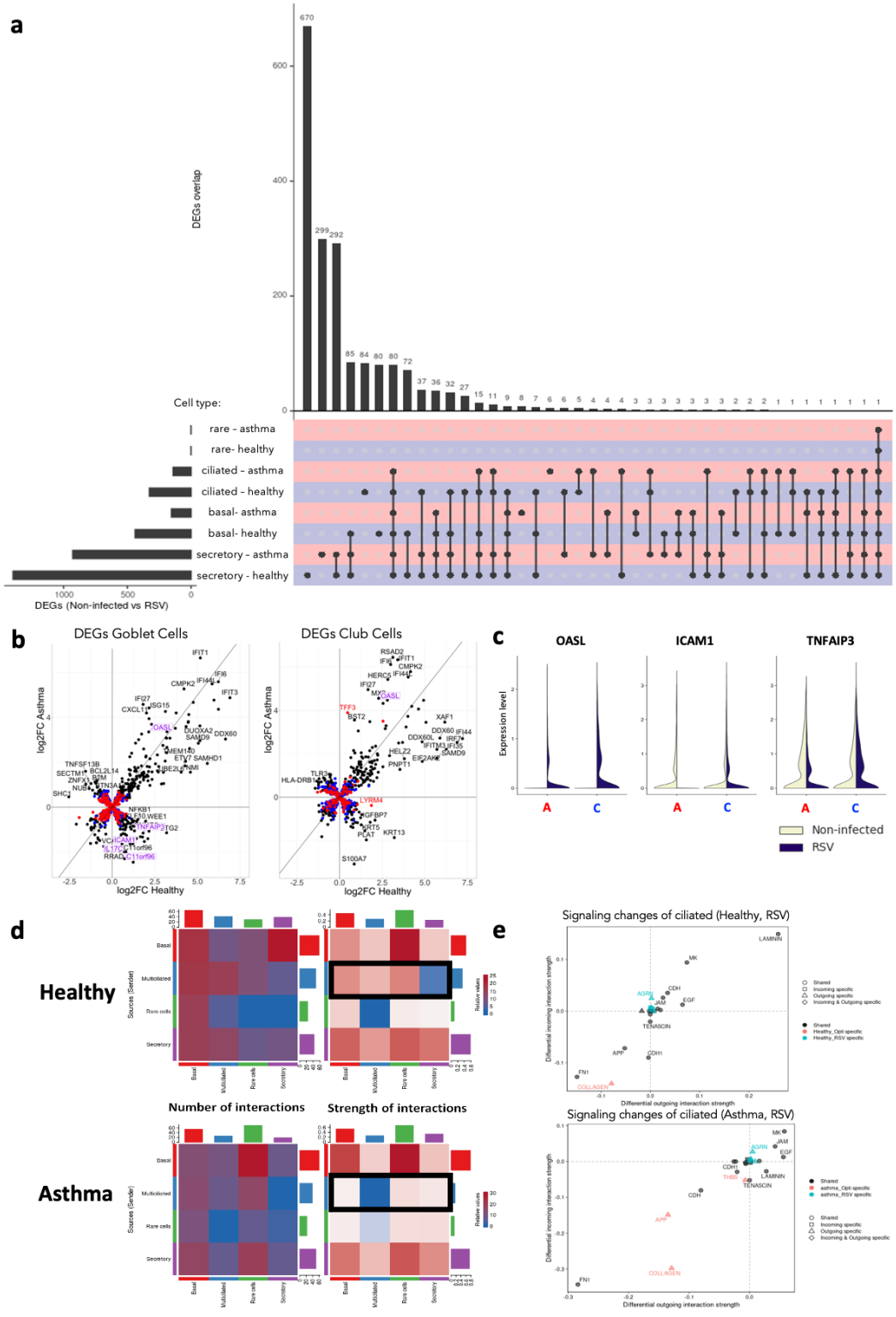

Figure 4 RSV infection induces a different transcriptomic response and a shift in cellular communication in pBECs derived from patients with asthma compared with control. (A) UpSet plot depicting the unique and shared sets of DEGs with RSV infection among cell types in control (blue) and in asthma (red). An FDR of less than 0.05 was considered as statistically significant. (B) Change in gene expression induced by RSV, for goblet (left) and club (right) cells. Only genes found to be significantly different in RSV (FDR <0.05) in either the healthy-derived or the asthma-derived pBECs are displayed. DEGs found in both conditions are coloured in black, DEGs only found in healthy (resp. asthma) are coloured in blue (resp. red). Genes found significant (FDR <0.05) in the interaction analysis are coloured in purple. (C) Violin plots of the expression of *OASL*, *ICAM1* and *TNFAIP3* in goblet cells derived from patients with asthma (A) and healthy controls (C). (D) Differential number and strength of cell–cell interactions when comparing untreated with RSV-infected cells derived from healthy subjects (top) and from patients with asthma (bottom). Red (or blue) depicts an increase (or decrease) of these metrics in the RSV-infected cells compared with untreated cells. (E) Signalling changes of multiciliated cells in control (top) and in asthma (bottom) when comparing untreated and RSV-infected samples. DEGs, differentially expressed genes; FDR, false discovery rate; pBECs, primary bronchial epithelial cells; RSV, respiratory syncytial virus.

In pBECs from asthma, the RSV-induced transcriptional response is largely similar to that of healthy-derived pBECs

Next, we assessed the response to RSV of the ALI cultures of pBECs derived from patients with asthma. For those, all 10 subtypes of pBECs were observed (online supplemental figure 4A), whereby RSV infection did not induce any significant changes in their relative proportions (online supplemental figure 4B). No significant changes in TEER or in the expression of genes involved in barrier formation were observed 72 hpi (online supplemental figure 2B,C).

To investigate the transcriptional response to RSV in asthma-derived pBECs, we performed DGE analysis per cell type. For all cell types, fewer DEGs were found in pBECs from patients with asthma than in those from healthy donors (figure 4A, online supplemental figure 4C and online supplemental table 3). However, similar to the healthy pBECs, the highest number of DEGs in asthma was detected in the transitory cells (online supplemental figure 4C). GO analysis of all the DEGs found for the basal, secretory and ciliated cells separately revealed an enrichment of biological processes involved in immune and antiviral responses (online supplemental figure 4D and online supplemental table 4). No biological processes were found to be exclusively enriched for the multiciliated cells in asthma. However—and similarly to what was observed in healthy—many metabolic processes were only found enriched in the secretory cells, and the processes related to lymphocyte-mediated immunity were exclusively being enriched in the basal cells.

In addition, an enrichment of major inflammatory pathways after RSV infection, including IFN-α response, IFN-γ response and NF-κB response, was observed (online supplemental figure 5A). At the protein level, quantification by ELISA revealed higher concentrations of IFN-λ-1/IFN-λ-3 in the apical washes of the RSV-infected 24 hpi and 48 hpi samples compared with the uninfected samples, for pBECs derived from both patients with asthma and healthy subjects, with no differences observed between these two groups. No differences in levels of IFN-β were detected (online supplemental figure 5B).

In asthma, the expression of several genes involved in the antiviral response is altered in goblet cells

By comparing the changes in gene expression induced with RSV between the healthy-derived cells and the asthma-derived cells, we observed several genes displaying an opposite change after RSV infection in asthma compared with healthy (figure 4B and online supplemental figure 6).

To determine which genes were significantly differentially regulated in response to RSV infection between pBECs from patients with asthma and those from healthy controls, we performed an interaction analysis per cell type (see online supplemental methods). We found a significant interaction for eight genes, six of which were observed in goblet cells (table 4). Of these, *OASL*, *ICAM1* and *TNFAIP3* display an impaired expression in asthma samples infected with RSV compared with control (figure 4B,C), with both *OASL* and *TNFAIP3* being more induced by RSV in the healthy goblet cells than in the goblet cells from asthma donors, and *ICAM1* not being induced by RSV in the goblet cells in asthma at all.

Change in cellular communication induced by RSV is impaired in asthma

Cell–cell communication analysis showed similar changes of behaviour with RSV in both asthma-derived and healthy-derived cells, with an increase in the number of interactions after RSV infection, but a decrease in the strength of those interactions (online supplemental figure 7A). Signals sent from multiciliated cells to secretory cells were increased and stronger with RSV for the healthy pBECs, but were decreased in asthma (figure 4D). For both groups, the outgoing collagen signalling from multiciliated cells was absent from the RSV-infected cells (figure 4E). Interestingly, APP (amyloid precursor protein) and THBS (thrombospondin) signalling, both found in the untreated and RSV-infected healthy multiciliated cells, were only detected in the untreated condition in asthma, but not in RSV-infected cells. In basal and in secretory cells, they were found in both untreated and RSV conditions (online supplemental figure 7B,C).

DISCUSSION

RSV plays a critical role in early-life recurrent wheeze and in asthma exacerbation. The response to RSV infection differs between the healthy and the asthma bronchial epithelium. In this study, we compared the transcriptome of bronchial epithelial cells from healthy and asthma donors in ALI cultures before and after RSV infection, to better understand the molecular and cellular mechanisms causing this difference. We found many similarities in the transcriptional response to RSV between pBECs of patients with asthma and pBECs of healthy donors, with an overlapping antiviral response across cell types. However, after RSV infection, the expression of genes involved in triggering the IFN response was lower in the goblet cells from the patients with asthma compared with those from healthy controls. In addition, the APP and the THBS signalling observed with RSV infection in control cultures were impaired in multiciliated cells after RSV infection in cultures from patients with asthma. Overall,

Table 4 Significant genes from the interaction term ($asthma_{RSV}$–$asthma_{mon\text{-}infected}$)–($healthy_{RSV}$–$healthy_{non\text{-}infected}$)

	Gene ID	Gene name	FDR	Direction of the change
Basal resting cells	CRCT1	Cysteine-rich C-terminal 1	0.042	RSV induced in asthma only
Cycling cells	KRT14	Keratin 14	0.011	RSV induced in healthy only
Goblet cells	ICAM1	Intercellular adhesion molecule 1	0.011	Increased RSV induction in healthy
	IL17C	Interleukin 17C	0.045	RSV induced in healthy only
	DUSP2	Dual specificity phosphatase 2	0.045	RSV induced in healthy only
	C11orf96	Chromosome 11 open reading frame 96	0.045	RSV induced in healthy only
	OASL	2′–5′-oligoadenylate synthetase like	0.045	RSV induced in healthy only
	TNFAIP3	Tumour necrosis factor alpha-induced protein 3	0.045	Increased RSV induction in healthy

Interaction analysis was performed using edgeR, for each cell type. Statistical significance was considered for genes with an FDR <0.05.
FDR, false discovery rate; RSV, respiratory syncytial virus.

our study indicates that the changes in the response to RSV in cultured airway epithelial cells in asthma are mostly observed to the most differentiated cells, suggesting that these would be preferred target cells for potential drug development.

Contrary to what others previously described, there was no reduction in TEER measurement caused by the RSV infection.[30] This could indicate that the RSV did not cause lysis of the cells in our model, and corroborates with previous studies where no obvious deterioration of ALI cultures was observed after RSV infection.[31] In addition, we did not observe any increase of mRNA expression encoding the viral receptors in asthma, in opposition to what was previously described.[9] In similar models, it was also originally suggested that RSV would preferentially infect ciliated cells.[31] Our data suggest that it is not the case, similarly to what others reported previously.[32] However, it is important to note that for some samples of our dataset, the number of ciliated cells was limited. In general, our model also presents some discrepancies with literature, as it does not reflect the expected[18] increase of mucus-producing cells in asthma.

In our study, the strong antiviral response after RSV infection presents similarities with the response to SARS-CoV-2 infection,[33] with goblet cells showing a strong inflammatory signature in both cases. *ICAM1* and *TNFAIP3*, known to be involved in the antiviral response, were previously identified as some of the best drug targets for COVID-19.[34] In our study, *ICAM1* and *TNFAIP3* have a lower expression in goblet cells in asthma in response to RSV. The relevance of studying goblet cells in respiratory viral infections has already been demonstrated for rhinovirus, multiple influenza viruses and hantavirus.[35] Recently, goblet cells were also found to play a critical role in SARS-CoV-2 infection in the lung, and an increased viral replication in the chronic obstructive pulmonary disease (COPD) airway epithelium was observed, likely due to COPD-associated goblet cell hyperplasia.[36] Our findings, taken together with the emerging role of goblet cells observed in recent literature, suggest that goblet cells play a critical role in RSV-induced asthma exacerbation. This highlights the need for deeper investigations of goblet cells, especially, in the context of airway diseases, frequently associated with goblet cell metaplasia and hyperplasia and for which antiviral response is impaired.

Overall, gaining insights at a cell type-specific level about the link between the epithelium and the activities of the immune cells seems to remain necessary for future development towards RSV-mediated asthma exacerbation.

Author affiliations
[1]Department of Pathology and Medical Biology, University of Groningen, University Medical Center Groningen, Groningen, the Netherlands
[2]GRIAC research institute, University Medical Center Groningen, Groningen, the Netherlands
[3]Department of Pulmonology, University of Groningen, University Medical Center Groningen, Groningen, the Netherlands
[4]Department of Pediatric Pulmonology and Pediatric Allergology, Beatrix Children's Hospital, University of Groningen, University Medical Center Groningen, Groningen, the Netherlands
[5]Department of Pediatric Infectious Diseases and Immunology, Wilhelmina Children's Hospital, University Medical Center Utrecht, Utrecht, the Netherlands
[6]Division of Infectious Diseases, Department of Pediatrics, University Medical Centre Utrecht, Utrecht, the Netherlands
[7]Department of Pulmonary Medicine, Erasmus University Medical Center, Rotterdam, the Netherlands

X Aurore C A Gay @Aurore__Gay

Acknowledgements The authors thank Uilke Brouwer, Sharon Brouwer, Marnix Jonker, Marissa Wisman and Jelmer Vlasma, from the Department of Pathology and Medical Biology of the University Medical Center Groningen, for their support in the experimental procedure. They also acknowledge Marijn Berg (University Medical Center Groningen), Alen Faiz (University of Technology Sydney) and Hana Aliee (Helmholtz Zentrum München) for their advice for conducting the bioinformatics analysis.This publication is part of the Human Cell Atlas - www.humancellatlas.org/publications.

Contributors ACAG performed the experiments, processed the experimental data, performed most of the analysis, drafted the manuscript and designed the figures. MB performed the preprocessing of the data and aided in the data analysis. OC, TMK and MvdB recruited the patients and performed the bronchoscopies. LA, DvG and PAF were involved in processing the raw samples and in the ELISA experiment. GHK, LB, RWH, MvdB and MCN were involved in interpretation of the results and the supervision of the work. MCN, RWH and MvdB conceived the project and secured project funding. MCN acts as guarantor for this study. All authors discussed the results and contributed to manuscript writing and revisions.

Funding Funded by H2020 Research and Innovation under the grant no 874656 and by the Netherlands Lung Foundation under the grants 4.1.18.226 and 5.1.14.020.

Competing interests GHK, MCN and MvdB received project funding from GlaxoSmithKline. GHK and MvdB received funding from AstraZeneca. MvdB received funding from Novartis, Genentech and Roche.

Patient consent for publication Not required.

Ethics approval The Medical Ethics Committee of University Medical Center Groningen (UMCG) approved the study and all subjects gave written informed consent.

Provenance and peer review Not commissioned; externally peer reviewed.

Data availability statement Data are available upon reasonable request. Count matrices are available on EGA. Full supplemental tables are available on https://discovair.org/data-sets.

ORCID iDs
Aurore C A Gay http://orcid.org/0000-0002-1593-2674
Orestes Carpaij http://orcid.org/0000-0001-9774-5743
Tessa M Kole http://orcid.org/0000-0002-5176-6300

REFERENCES

1 Lundbäck B, Backman H, Lötvall J, *et al*. Is asthma prevalence still increasing *Expert Rev Respir Med* 2016;10:39–51.
2 Ramsahai JM, Hansbro PM, Wark PAB. Mechanisms and management of asthma exacerbations. *Am J Respir Crit Care Med* 2019;199:423–32.
3 Westerly BD, Peebles RS. Respiratory syncytial virus infections in the adult asthmatic – mechanisms of host susceptibility and viral subversion. *Immunol Allergy Clin North Am* 2010;30:523–39,
4 Hackett T-L, Singhera GK, Shaheen F, *et al*. Intrinsic phenotypic differences of asthmatic epithelium and its inflammatory responses to respiratory syncytial virus and air pollution. *Am J Respir Cell Mol Biol* 2011;45:1090–100.
5 Xiao C, Puddicombe SM, Field S, *et al*. Defective epithelial barrier function in asthma. *J Allergy Clin Immunol* 2011;128:549–56.
6 Bonser LR, Erle DJ. The airway epithelium in asthma. *Adv Immunol* 2019;142:1–34.
7 Shikhagaie MM, Andersson CK, Mori M, *et al*. Mapping of TLR5 and TLR7 in central and distal human airways and identification of reduced TLR expression in severe asthma. *Clin Exp Allergy* 2014;44:184–96.
8 Patella V, Bocchino M, Steinhilber G. Asthma is associated with increased susceptibility to infection. *MINERVA Med* 2015;106:1–7.
9 Farne HA, Johnston SL. Immune mechanisms of respiratory viral infections in asthma. *Curr Opin Immunol* 2017;48:31–7.
10 Battles MB, McLellan JS. Respiratory syncytial virus entry and how to block it. *Nat Rev Microbiol* 2019;17:233–45.

11 Lay MK, González PA, León MA, *et al*. Advances in understanding respiratory syncytial virus infection in airway epithelial cells and consequential effects on the immune response. *Microbes Infect* 2013;15:230–42.
12 Wark PAB, Johnston SL, Bucchieri F, *et al*. Asthmatic bronchial epithelial cells have a deficient innate immune response to infection with rhinovirus. *J Exp Med* 2005;201:937–47.
13 Edwards MR, Regamey N, Vareille M, *et al*. Impaired innate interferon induction in severe therapy resistant Atopic asthmatic children. *Mucosal Immunol* 2013;6:797–806.
14 Parsons KS, Hsu AC, Wark PAB. TLR3 and MDA5 signalling, although not expression, is impaired in asthmatic epithelial cells in response to rhinovirus infection. *Clin Exp Allergy* 2014;44:91–101.
15 Baraldo S, Contoli M, Bazzan E, *et al*. Deficient antiviral immune responses in childhood: distinct roles of atopy and asthma. *J Allergy Clin Immunol* 2012;130:1307–14.
16 Patel DA, You Y, Huang G, *et al*. Interferon response and respiratory virus control are preserved in bronchial epithelial cells in asthma. *J Allergy Clin Immunol* 2014;134:1402–12.
17 Veerati PC, Troy NM, Reid AT, *et al*. Airway epithelial cell immunity is delayed during rhinovirus infection in asthma and COPD. *Front Immunol* 2020;11:974.
18 Vieira Braga FA, Kar G, Berg M, *et al*. A cellular census of human lungs identifies novel cell States in health and in asthma. *Nat Med* 2019;25:1153–63.
19 Berg M, Petoukhov I, van den Ende I, *et al*. FastCAR: fast correction for ambient RNA to facilitate differential gene expression analysis in single-cell RNA-sequencing datasets. *Bioinformatics* [Preprint] 2022.
20 Hao Y, Hao S, Andersen-Nissen E, *et al*. Integrated analysis of multimodal single-cell data. *Cell* 2021;184:3573–87.
21 Heaton H, Talman AM, Knights A, *et al*. Souporcell: robust clustering of single-cell RNA-Seq data by genotype without reference Genotypes. *Nat Methods* 2020;17:615–20.
22 Haghverdi L, Lun ATL, Morgan MD, *et al*. Batch effects in single-cell RNA-sequencing data are corrected by matching mutual nearest neighbors. *Nat Biotechnol* 2018;36:421–7.
23 Büttner M, Ostner J, Müller CL, *et al*. scCODA is a Bayesian model for compositional single-cell data analysis. *Nat Commun* 2021;12:6876.
24 Robinson MD, McCarthy DJ, Smyth GK. edgeR: a bioconductor package for differential expression analysis of digital gene expression data. *Bioinformatics* 2010;26:139–40.
25 Jin S, Guerrero-Juarez CF, Zhang L, *et al*. Inference and analysis of cell-cell communication using Cellchat. *Nat Commun* 2021;12:1088.
26 Ruiz García S, Deprez M, Lebrigand K, *et al*. Novel dynamics of human mucociliary differentiation revealed by single-cell RNA sequencing of nasal epithelial cultures. *Development* 2019;146:dev177428.
27 Griffiths CD, Bilawchuk LM, McDonough JE, *et al*. IGF1R is an entry receptor for respiratory syncytial virus. *Nature* 2020;583:615–9.
28 Asgari S, Schlapbach LJ, Anchisi S, *et al*. Severe viral respiratory infections in children with IFIH1 loss-of-function mutations. *Proc Natl Acad Sci U S A* 2017;114:8342–7.
29 de Vries M, Nwozor KO, Muizer K, *et al*. The relation between age and airway epithelial barrier function. *Respir Res* 2022;23:43.
30 Rezaee F, DeSando SA, Ivanov AI, *et al*. Sustained protein kinase D activation mediates respiratory syncytial virus-induced airway barrier disruption. *J Virol* 2013;87:11088–95.
31 Villenave R, Shields MD, Power UF. Respiratory syncytial virus interaction with human airway epithelium. *Trends Microbiol* 2013;21:238–44.
32 Persson BD, Jaffe AB, Fearns R, *et al*. Respiratory syncytial virus can infect basal cells and alter human airway epithelial differentiation. *PLoS ONE* 2014;9:e102368.
33 Yoshida M, Worlock KB, Huang N, *et al*. Local and systemic responses to SARS-CoV-2 infection in children and adults. *Nature* 2022;602:321–7.
34 Islam T, Rahman MR, Aydin B, *et al*. Integrative transcriptomics analysis of lung epithelial cells and identification of repurposable drug candidates for COVID-19. *Eur J Pharmacol* 2020;887:173594.
35 Cortez V, Schultz-Cherry S. The role of goblet cells in viral pathogenesis. *FEBS J* 2021;288:7060–72.
36 Osan JK, Talukdar SN, Feldmann F, *et al*. Goblet cell hyperplasia increases SARS-Cov-2 infection in COPD. *bioRxiv* 2020:2020.11.11.379099.

Supplementary Material

Material and methods

Primary cell culture and RSV infection

Patient recruitment and ethical approval

As described previously (Vieira Braga et al., 2019), all subjects were included using the following criteria: age range from 40 to 65 years old, and a history of smoking<10 pack-years. In addition, control subjects had to meet the following inclusion criteria: absent history of asthma, no use of asthma-related medication, a negative provocation test (i.e. PC20 methacholine >8mgml−1, and adenosine 5′-monophosphate >320mgml−1 with 2min protocol), no pulmonary obstruction (i.e. FEV1/forced vital capacity (FVC)≥70%) and absence of lung function impairment (that is FEV1≥80% predicted). As for the asthma patients, the criteria essential for inclusion were the following: age of onset of asthma symptoms ≤12 years old, documented history of asthma, use of inhaled corticosteroids with(out) β2-agonists due to respiratory symptoms, and a positive provocation test (that is, PC20 methacholine (concentration of methacholine needed to produce a 20% fall in the forced expiratory volume in the first second (FEV1)) ≤ 8mgml−1 with 2min protocol). Six weeks before all tests, the asthma patients stopped inhaled corticosteroids. All subjects were clinically characterized with pulmonary function and provocation tests and underwent a fibreoptic bronchoscopy under conscious sedation according to a standardized protocol. The bronchoscopy was postponed for ≥6 weeks for subjects who developed upper respiratory symptoms. For this study, macroscopically adequate endobronchial brushes, located between the third and sixth generation of the right lower and middle lobe, were collected. Extracted brushes were placed in HBSS (Lonza) supplemented with 10% Penicilin (10000U/mL)/Streptomycin (10000ug) (Gibco) and kept on ice before being processed within 1 hour. This study was approved by the medical ethics committee of the University Medical Center Groningen, and all subjects gave their written informed consent.

Coating

All flasks and transwell inserts were coated at 37°C overnight with EMEM (BE12-709F, Lonza) supplemented with 0,1% BSA (A2058-1G, Sigma), 1% fibronectin (F-11415MG, Sigma) and 1% PureCol^{TM} (#5005, CellSystems), prior to seeding the cells.

Expansion of the pBECs in culture

Cells were cultured and expanded as previously described [18]. Briefly, cells were pelleted at 500g for 10 minutes, and both the cells pellet and the brushes were transferred into a coated T12,5cm2 culture flask (#350318, Corning). Cells were cultured at 37°C in a humidified atmosphere of 5% CO2. Airway Epithelial Cell Growth medium (#C39165, Sigma), supplemented with 1% Penicillin-Streptomycin (#15140-122, Gibco) and supplement mix (ref) was used for the culture and refresh regularly. After reaching confluency passage, cells were washed twice with HBSS (BE10-543F, Lonza) and incubated for 5 minutes in trypsin-EDTA (0.25%) (Gibco). The reaction was stopped using an equal volume of heated-inactivated-FCS (F7524, Sigma-Aldrich), and cells were pelleted at 500g during 5 minutes before being resuspended in BEGM+10% DMSO (#D2650, Sigma). Cells were cryopreserved overnight at -80 and stored in liquid nitrogen. Cryopreserved cells were thawed at 37°C, and 15mL of warm HBSS was added dropwise to the cell suspension. After pelleting the cells for 5 minutes at 200g, supernatant was discarded and cells were resuspended in 5mL of BEGM and transferred into coated T25cm2 culture flasks (#430372, Corning) and expanded (87,500 cells per T25cm2

flasks). After a total of two passages post-thawing, cells were seeded into transwell inserts (CLS-3470, Corning) for ALI culture.

ALI culture and infection

The pBECs were cultured at air-liquid interface conditions as previously described (Burgess et al., 2021). Briefly, 75,000 cells were seeded into a coated 6.5mm with 0.4 µm Pore Polyester Membrane transwell insert (CLS-3470, Corning), and cultured with 500uL of BEGM in the basolateral side, and 200uL BEGM in the apical side. After reaching confluency, cells were exposed to air by removing the medium from the apical part and replacing the medium in the basolateral part with a 1:1 mix of AEBM (C-21260, Promocell) and DMEM (BE12-709F, Lonza), supplemented with Airway Epithelial Cell Growth Medium (#C39165, Merck), 1% Penicillin-Streptomycin (#15140-122, Gibco), BSA (1.5 µg/ml; A2058-1G, Sigma), and retinoic acid (RA, 15 ng/ml; R2625, Sigma). The medium was changed three times a week. Barrier formation of the cultures was monitored by measuring the transepithelial electrical resistance (TEER) using the Millicell ERS-2 Voltohmmeter (MERS00002, Merck), according to manufacturer's instructions. During the fourth week of culture, cells were infected by apical exposure to RSV strain A at $3.5x10^7$ PFU/mL (or control condition) in OptiMEM (Gibco), for 2 hours at 37°C, followed by removal of the Optimem. Cells were harvested 72 hours after infection, using tripLE (Gibco) and trypsin-EDTA (0.25%) (Gibco) before being processed for scRNAseq.

Protein quantification

For ELISA, apical washes were obtained by washing apical parts of the inserts with 100 µL of OptiMEM at 8-, 24-, 48-, and 72-hpi. Human IFN-beta Quantikine ELISA Kit (R&D Systems, USA) and Human IL- 29/IL-28B (IFN-lambda 1/3) DuoSet ELISA Kit (R&D Systems, USA) were used according to the manufacturer's recommendations.

Computational analysis

Clustering and annotations

To annotate the scRNAseq dataset, we used an iterative clustering analysis approach. For the level 2 annotations, the cells from the RSV samples were annotated separately from the cells from the non-infected samples. For each iteration, the highest granularity of clustering not resulting in subject-driven clusters was used.

Supplementary figures

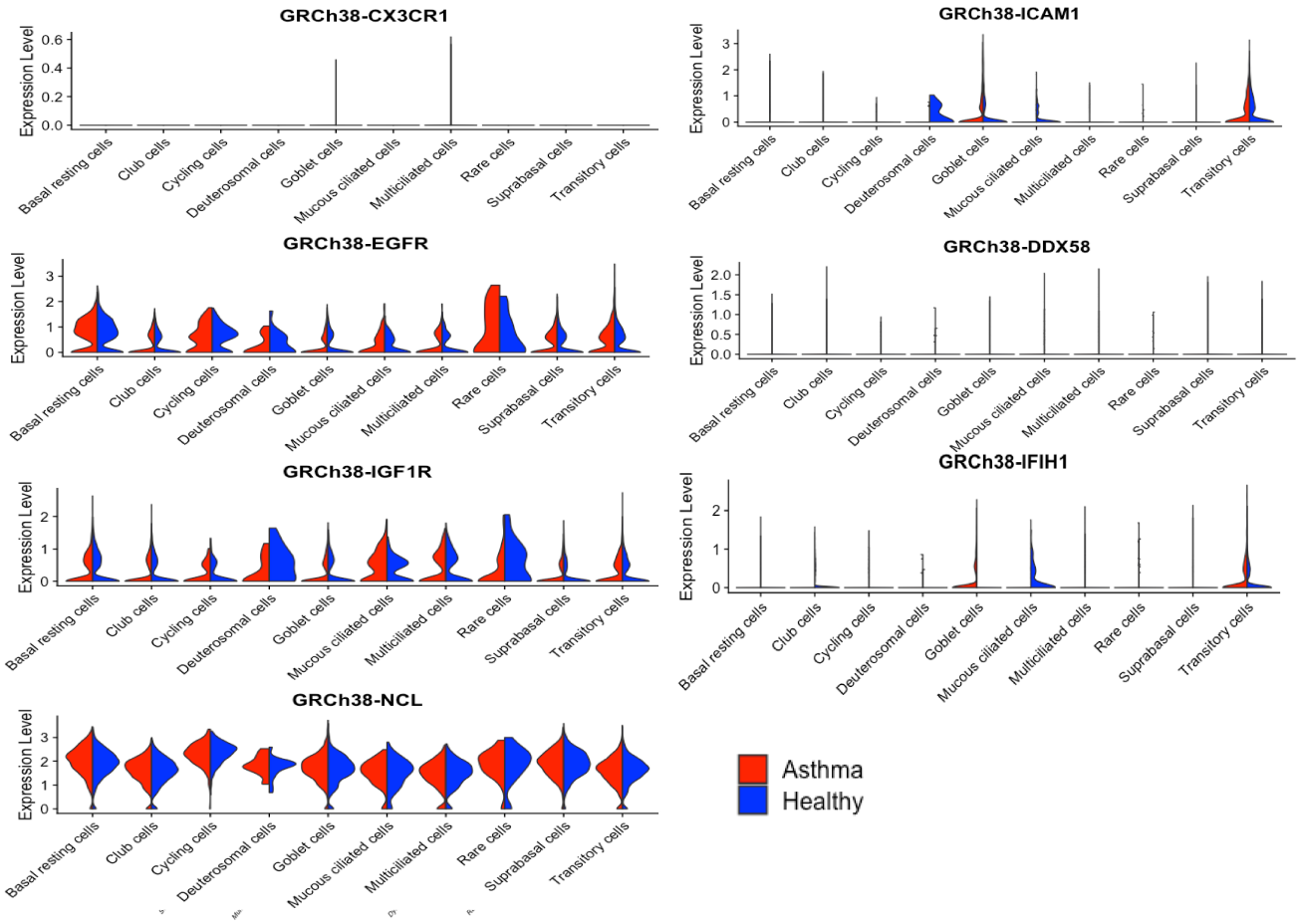

Supplementary figure 1: ALI cultures of pBECs derived from healthy donors and asthma patients show similar expression of the RSV receptors. Violin plots of the expression of RSV receptors for the non-infected samples. Differential gene expression between the two groups was performed in each cell type. A FDR of less than 0.05 was considered statistically significant.

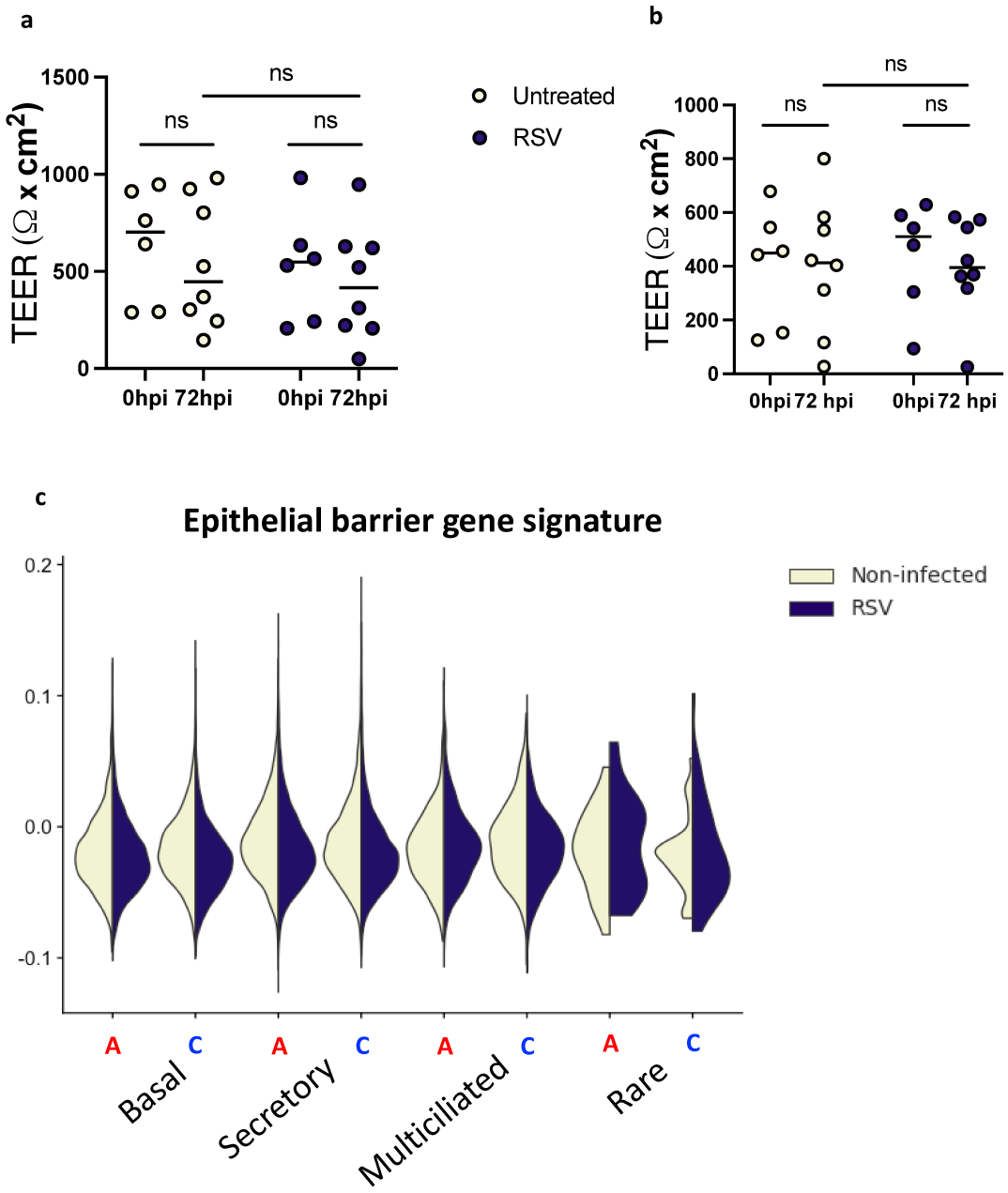

Supplementary figure 2: RSV infection does not alter the epithelial barrier. Comparison at 72hpi of the TEER measurements of the untreated and the RSV infected ALI cultures of pBECS derived from (**a**) control and (**b**) asthma donors. (**c**) Violin plots of the composite score of the genes involved in the epithelial barrier formation in the pBECs derived from asthma patients (**A**) and healthy controls (**C**).

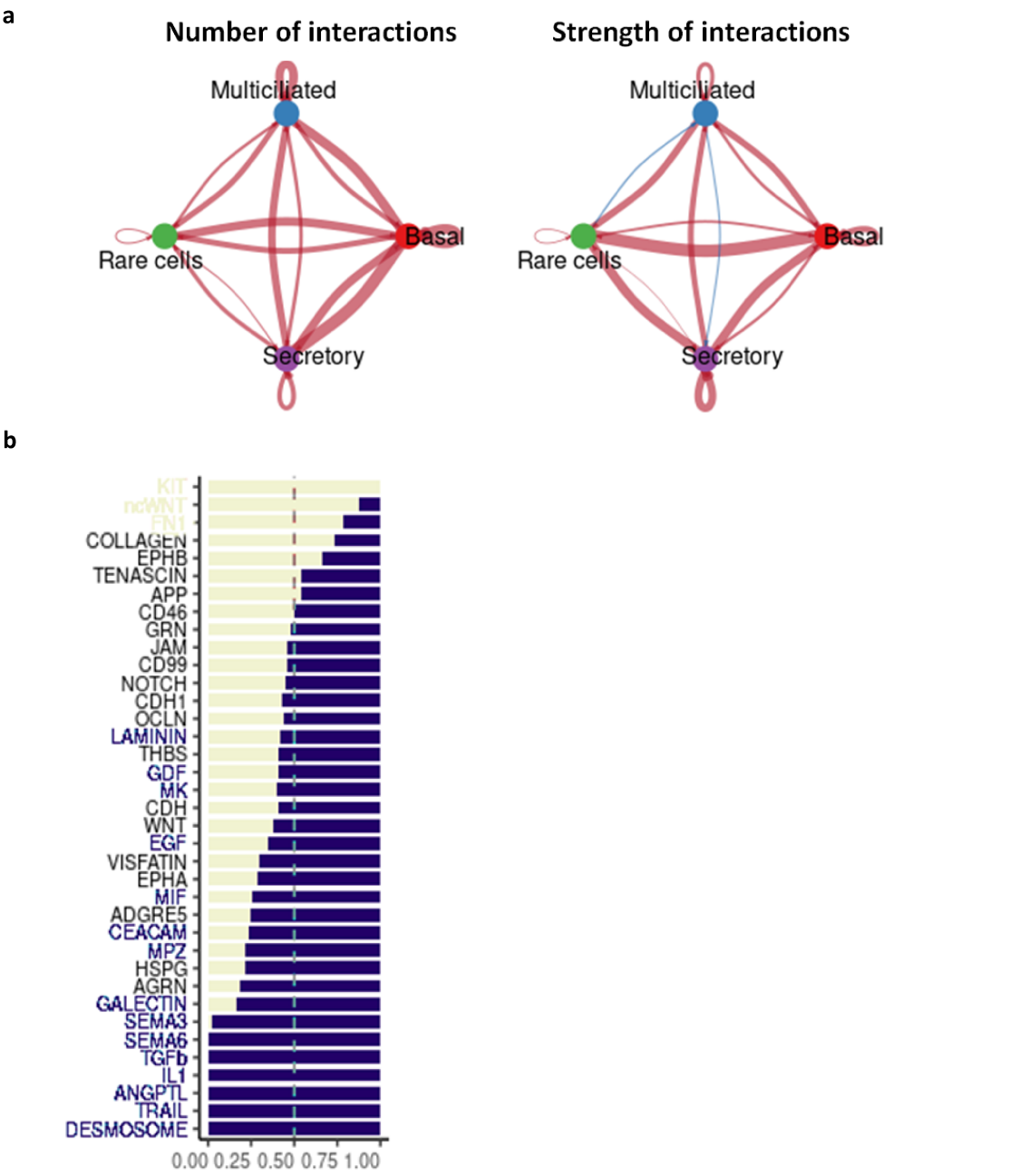

Supplementary figure 3: RSV induces a shift in cell-cell communication in the healthy-derived pBECs. (**a**) Differential number (left) and strength (right) of cell-cell interactions, when comparing untreated to RSV infected cells. Nodes indicate cell type and edges thickness represents the relative interaction count or interaction strength. Edges colored in red (or blue) depicts an increase (or a decrease) of these metrics in the RSV infected cells compared to untreated cells. (**b**) Significant signaling pathways (right) ranked based on differences in the overall information flow within the inferred networks, when comparing untreated to RSV infected cells. Pathways in beige (or blue) indicate a significant enrichment in the non-infected (or RSV) condition, determined by CellChat.

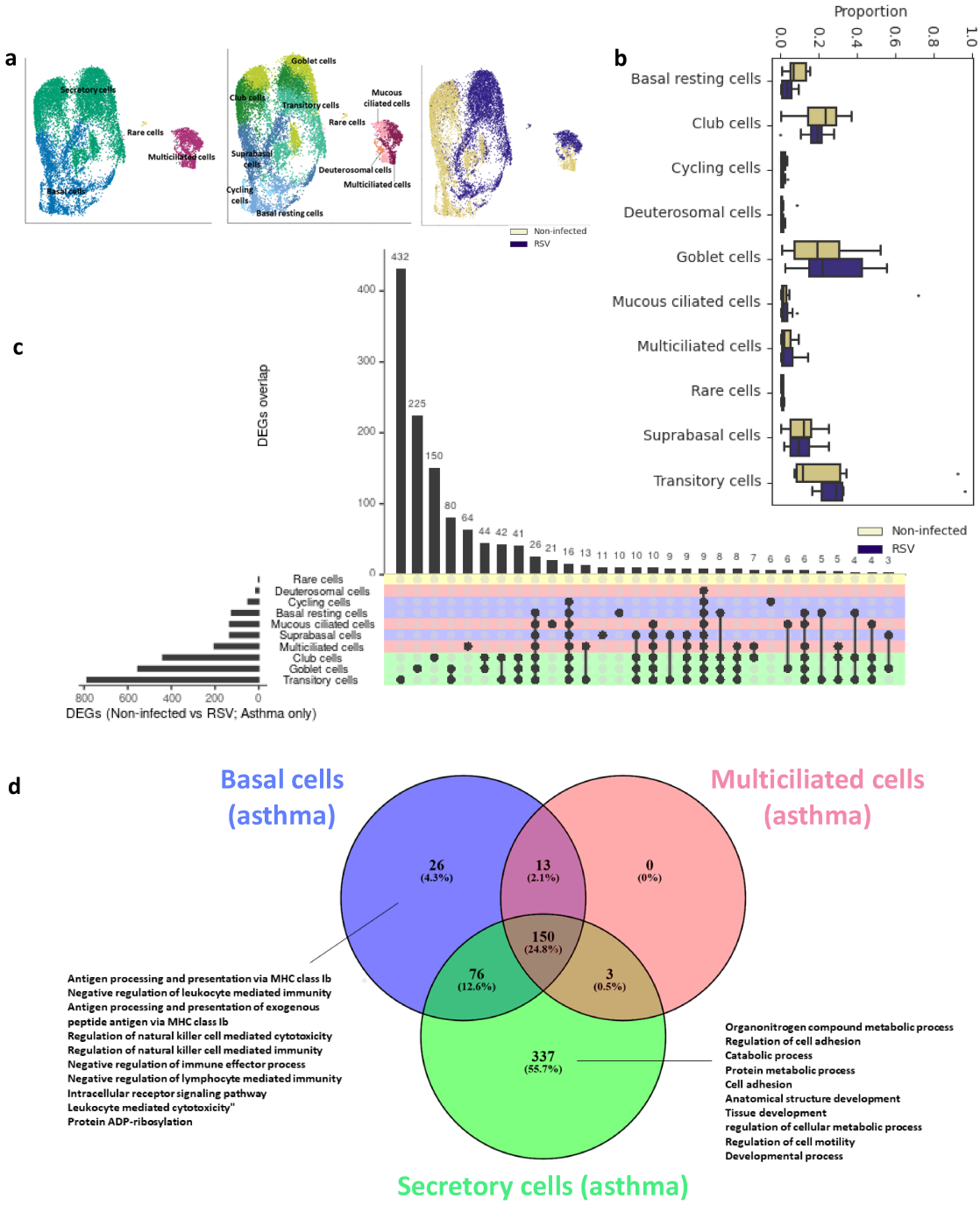

Supplementary figure 4: RSV response in asthma (**a**) UMAP representation of untreated 6,382 from untreated and 7,934 RSV-infected cells, colored by cell type (left), subtype (middle) and treatment (right). (**b**) Cellular frequencies of each cell subtype, colored by treatment. Significance was determined by scCODA with an FDR adjusted p-value <0.05. (**c**) UpSet plot depicting the unique and shared sets of DEGs with RSV infection among cell types. A FDR of less than 0.05 was considered as statistically significant. (**d**) Venn diagram of the biological processes found to be significantly enriched by GO analysis of the genes differentially expressed in RSV compared to control, in basal, secretory and multiciliated cells. The 10 most enriched processes are indicated.

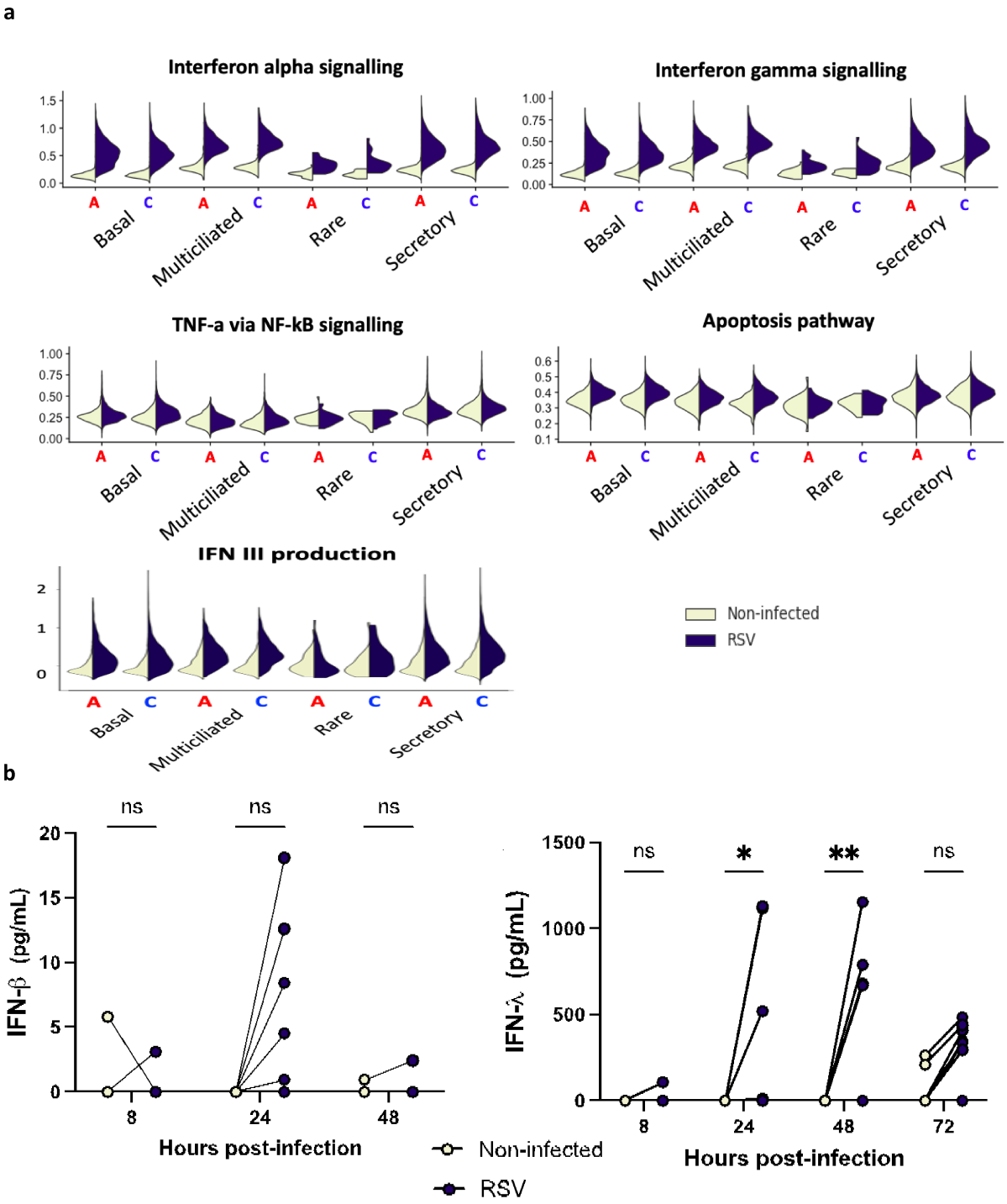

Supplementary figure 5: RSV infection induces an antiviral response in ALI cultures of pBECs derived from both control and asthma donors. (**a**) Violin plots of the composite score of the main antiviral response pathways in the pBECs derived from asthma patients (**A**) and healthy controls (**C**). (**b**) Concentration of IFN-ß and IFN-λ 1/3 measured by ELISA in the apical washes at different time points after infection for samples derived from both subjects with asthma (n=2) and healthy controls (n=3) combined, as no differences were observed between the two groups. *: p<0.05, **: p<0.01 (between the indicated values, as analyzed by the two way ANOVA test).

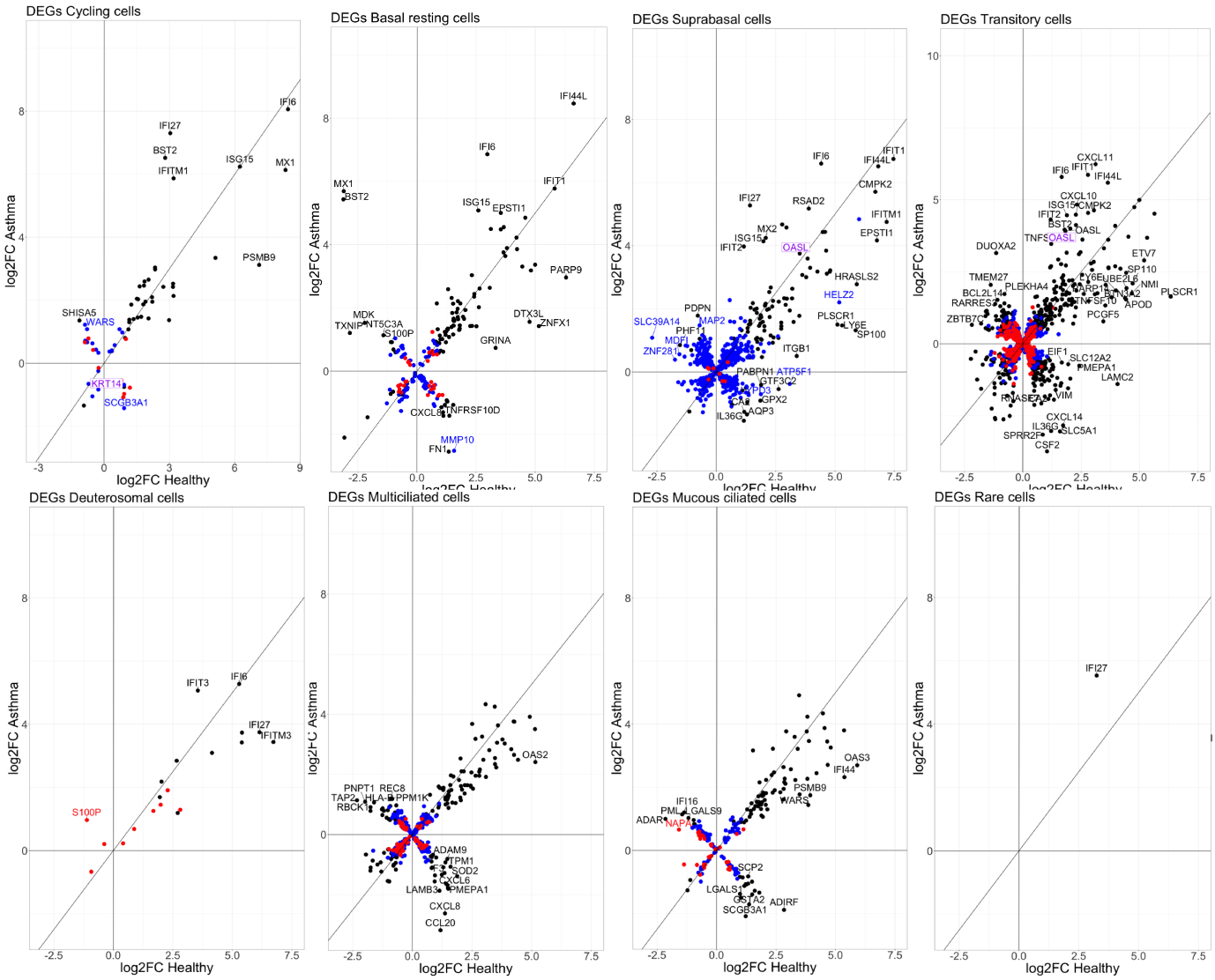

Supplementary figure 6: Effect of RSV on gene expression of pBECs derived from asthma patients compared to pBECs derived from healthy donors. The logFoldChange (log2FC) for the change in gene expression induced by RSV in healthy vs in asthma, for each cell type is represented. Only genes found to be significanty different in RSV (FDR<0.05) in either the healthy- or the asthma-derived pBECs are displayed. DEGs found in both conditions are colored in **black**, DEGs only found in healthy (resp. asthma) are colored in **blue** (resp. **red**). Genes found significant in the interaction analysis are colored in purple.

a

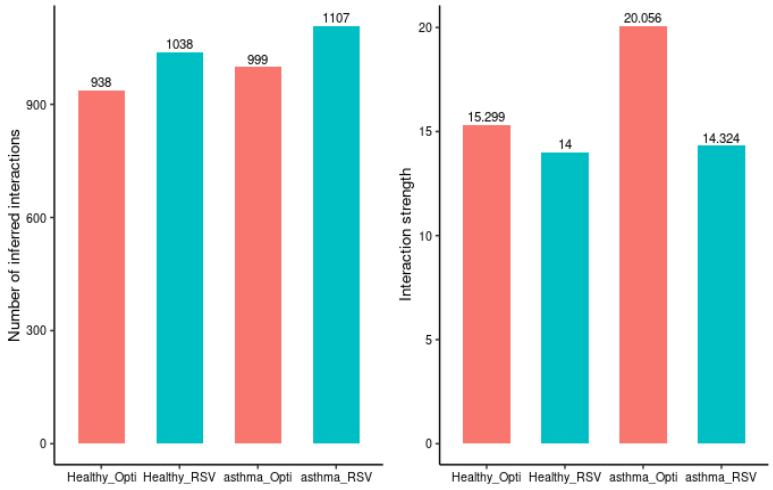
Number of inferred interactions
938
1038
999
1107
Healthy_Opti
Healthy_RSV
asthma_Opti
asthma_RSV
Interaction strength
15.299
14
20.056
14.324

b

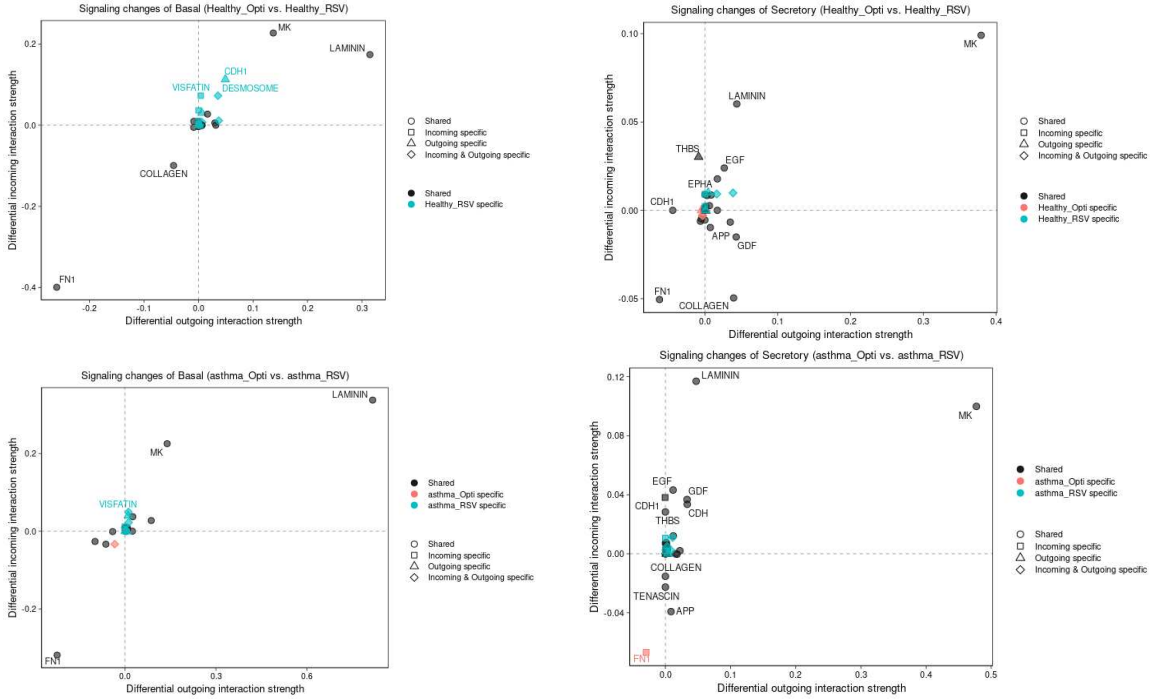
Signaling changes of Basal (Healthy_Opti vs. Healthy_RSV)
Differential incoming interaction strength
Differential outgoing interaction strength
MK
LAMININ
CDH1
VISFATIN
DESMOSOME
COLLAGEN
FN1
Shared
Incoming specific
Outgoing specific
Incoming & Outgoing specific
Healthy_RSV specific
Signaling changes of Secretory (Healthy_Opti vs. Healthy_RSV)
LAMININ
THBS
EGF
EPHA
CDH1
APP
GDF
FN1
COLLAGEN
Healthy_Opti specific
Signaling changes of Basal (asthma_Opti vs. asthma_RSV)
asthma_Opti specific
asthma_RSV specific
Signaling changes of Secretory (asthma_Opti vs. asthma_RSV)
EGF
GDF
CDH1
CDH
THBS
TENASCIN

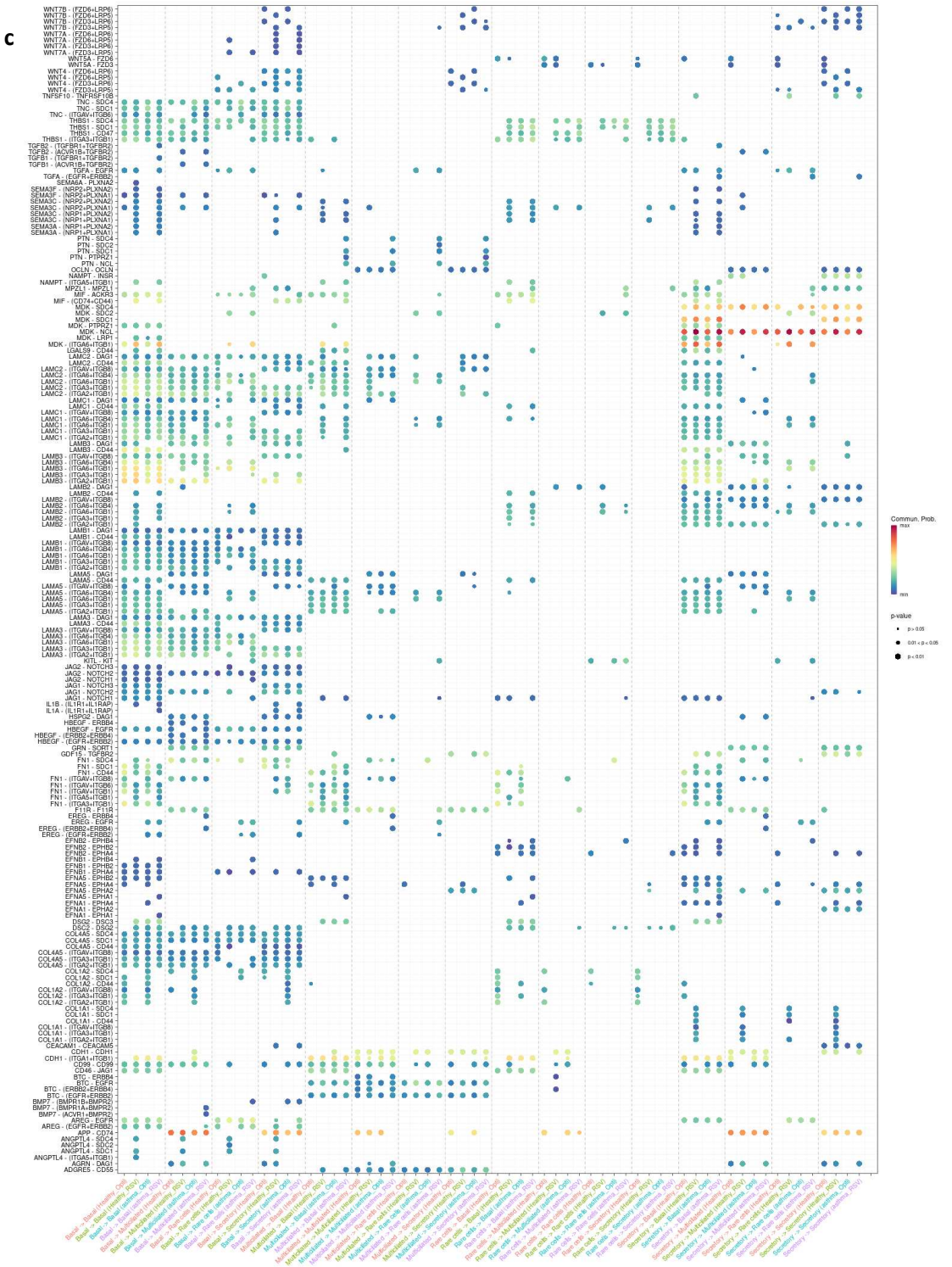

Supplementary figure 7: Cell-cell communication changes induced by RSV differ between asthma and control. (**a**) Number (left) and strength of inferred cellular interaction in untreated and RSV infected cells in asthma- and healthy-derived pBECs, determined with CellChat. (**b**) Signaling changes of basal (left) and secretory (right) in control (top) and in asthma (bottom) when comparing untreated and RSV infected samples. (**c**) Communication probabilities mediated by ligand-receptor pairs from some cell groups to other cell group.